



Identification of flavone and flavanone from ethyl acetate fraction of *Caesalpinia sappan* heartwood and tentative structure-activity relationship: An *in vitro* and *in silico* approach

Andrian Suchahyo¹, Moh. Farid Rahman¹, Husnul Khotimah², Widodo Widodo³, Siti Mariyah Ulfa¹ * 

¹Department of Chemistry, Faculty of Science, Brawijaya University, Malang, Indonesia.

²Department of Pharmacology, Faculty of Medicine, Brawijaya University, Malang, Indonesia.

³Department of Biology, Faculty of Science, Brawijaya University, Malang, Indonesia.

ARTICLE INFO

Received on: 07/03/2023

Accepted on: 21/08/2023

Available Online: 04/11/2023

Key words:

Flavonoid, flavone, flavanone, oxidative reaction, DPPH, molecular docking.

ABSTRACT

Caesalpinia sappan, commonly known as secang in Indonesia, has been used in traditional medicine to treat inflammation, microbial infection, diabetes, and cancer. In this study, the chromatographic separation of the ethyl acetate fraction of *C. sappan* was carried out. It resulted in the isolation of 2',5,6-trimethoxyflavone (TM) and cirsimaritin (CR), pinostrobin (PN), naringenin-5-methyl ether (NR), and alpinone (AL). All the compounds were elucidated and confirmed by LC-QToF-MS/MS. The *in vitro* antioxidant activity carried out by the 2,2-diphenyl-1-picrylhydrazyl method showed that all the compounds have potency as antioxidants. The tendency of antioxidative strength calculated from the ease of hydrogen transfer by density functional theory showed the activity order as follows: NR > PN > AL for subgroups of flavanone and CR > TM for subgroups of flavone, which have the same order as the *in vitro* result. *In silico* structure-activity relationships for the binding compounds to cytochrome P450 (CP450), lipoxygenase (LO), NADPH oxidase (NO), and xanthine oxidase (XO) were analyzed using the molecular docking and molecular dynamics techniques. The result revealed that the hydroxyl group of NR at the C-7 and C-4' positions is crucial to interact with Val113 and Asn217 in the CP450. Furthermore, the absence of the hydroxyl group at the C-3 position of PN shows better binding energy ($\Delta G = -4.05$ kcal/mol) compared to AL ($\Delta G = -1.7$ kcal/mol) in the LO. Double bonds at the C-2 and C-3 positions maintain the interaction with Asp179 of the NO receptor. For the XO receptor, two methoxy groups at the C-6 and C-5 positions (TM) are important to interact with a key residue like Arg880. Taken together, the result suggests that the flavone and flavanone derivatives from *C. sappan* have a potent antioxidant activity that could be useful in combating oxidative stress in the human body.

INTRODUCTION

Reactive oxygen species (ROS) is a byproduct generated in the mitochondrial respiratory chain by oxidative reactions (He *et al.*, 2017). A fair amount of ROS in our body is beneficial in killing pathogens and promoting wound healing by enhancing our immune system (Dhahri *et al.*, 2022). Nevertheless, excessive

production of ROS in the body can lead to oxidative damage to an intracellular cell, known as oxidative stress (Yang and Lian, 2020). Oxidative stress can cause damage to lipids, proteins, and DNA and promote various illnesses, including cancer, respiratory, cardiovascular, neurodegenerative, and digestive diseases (Liu *et al.*, 2018). Antioxidant enzymes such as superoxide dismutase, catalase, glutathione peroxidase, and glutathione reductase protect cells from oxidative stress (Qureshi *et al.*, 2022). External factors like tobacco smoke, air pollutants, and xenobiotics also promote oxidative stress (Bhattacharyya *et al.*, 2014). Those antioxidant enzymes are not enough to protect our cells. Therefore, exogenous antioxidant constituents are essential for quenching free radicals (Pham-Huy *et al.*, 2008).

*Corresponding Author

Siti Mariyah Ulfa, Department of Chemistry, Faculty of Science, Brawijaya University, Malang, Indonesia.
E-mail: ulfa.ms@ub.ac.id

Caesalpinia sappan, commonly known as secang by Indonesians, has been used as traditional medicine. Not only does secang have antioxidant activity, but it also has analgesic, antidiabetes, anti-inflammatory, antimicrobial, and anticancer activities (Annamalai *et al.*, 2019; Lim *et al.*, 2007; Mueller *et al.*, 2016; Naik Bukke *et al.*, 2018; Nirmal and Panichayupakaranant, 2015). Methanol, ethyl acetate, and water extracts of *C. sappan* have been reported to have antioxidant activity against the free radical 2,2-diphenyl-1-picrylhydrazyl (DPPH) (Badami *et al.*, 2003). Among the plant extracts, the most active ethyl acetate fraction is our scope of interest because it is predicted to have many active constituents that suppress oxidative stress.

Flavonoids play a defensive role in the plant against oxidative stress obtained by the plant's exposure to any of the abiotic stress (Mohammed, 2020). In animals and humans, flavonoids are unique compounds that have good antioxidant activity, either by hydrogen atom transfer (HAT) or by single electron transfer mechanism (Tatipamula and Kukavica, 2021). Flavonoid compounds such as protosappanin A and brazilin, isolated from *C. sappan*, have better antioxidant activities than vitamin E (Putri *et al.*, 2021). Brazilin was also found in *C. sappan* extract and showed to have antioxidant activity using ABTS⁺ test with an EC₅₀ of 26.5 μM, which is similar to Trolox (25.0 μM) (Liang *et al.*, 2013). Among flavonoid classes, flavone and flavanone have unique skeletons, that is, having a double bond at C2=C3 for flavone but not for flavanone. The other differences are the substituents attached to the core flavonoid ring. The reported flavones isolated from this plant were rhamnetin and quercetin (Cuong *et al.*, 2012; Shu *et al.*, 2008). Naringenin (NR) was the only identified flavanone from the *C. sappan* ethanolic fraction (Arjin *et al.*, 2021).

Cytochrome P450 (CP450), lipoxygenase (LO), NADPH oxidase (NO), and xanthine oxidase (XO) are known enzymes to generate ROS. Structure-activity relationship (SAR) gives a deeper insight into the inhibition mode of flavonoids and the derivatives against those macromolecules. For instance, a double bond between C2=C3 and hydroxyl groups at the C5 and C7 positions in flavone results in better inhibition toward XO. Moreover, the double bond in flavone also gives it a higher inhibitory activity against LO. The location of OH groups in flavonoids also affects their inhibition of the prooxidant enzymes (Amić *et al.*, 2007).

Therefore, flavone and flavanone in the ethyl acetate fraction of *C. sappan* are important constituents to be determined. In this research, the isolation and structure determination of flavone and flavanone derivatives from *C. sappan* were identified using liquid chromatography mass spectrometry (LC-MS)/QToF. *In vitro* and *in silico* analysis for each isolated component suggested that the kinds of substituents attached to the core structure of flavonoids influence the activity.

MATERIAL AND METHODS

Extraction and fractionation of *C. sappan*

Dry *C. sappan* heartwood simplicia collected from Malang, Indonesia, was purchased from Materia Medica, Batu, Malang, and authenticated as secang by Unit Pelaksana Teknis Materia Medica. The voucher sample was deposited in the Brawijaya University Herbarium of Microbiology Laboratory

under code number 191113.SCG H.001. A 300 g of *C. sappan* refluxed with MeOH (volume of MeOH is 5 times dried weight) for 1 hour. The extraction was repeated four times until the bright color of the extract faded. The concentrated MeOH extract under vacuum gave crude extract as a dark red solid (10.2% yield). Crude MeOH extract was partitioned using ethyl acetate according to Ulfa's *et al.* (2022) protocols as follows. The MeOH extract was resuspended in water with the ratio of extract and water 1:10 (w/v). The solution was then transferred in the separatory funnel and added with ethyl acetate in the ratio of 1:1 (v/v). The partition was carried out four times until the color of the solution faded. The ethyl acetate fraction was collected from the upper layer, separated, and evaporated using a vacuum. From 30.61 g of MeOH extract, the obtained ethyl acetate fraction was 22.64 g (74%).

Ten grams of the ethyl acetate fraction was purified using a silica gel column and eluted with a gradient solvent (CHCl₃: EtOAc, 6:4 to 0:1), giving ethyl acetate fraction (fraction A) (Ningsih *et al.*, 2020). Fraction A was purified further to get A1–A11 using stepwise gradient elution (CHCl₃: EtOAc = 6:4 to 0:1). Subfraction A3 was purified using the gradient solvent EtOAc: n-hexane 2:8 to 1:0 (v/v), which gave A3.3 as 2',5,6-trimethoxyflavone (TM) and A3.4 as cirsimaritin (CR). Subfraction A4 was purified using EtOAc:n-hexane 7:3 to 1:0 (v/v) to get A4.1–A4.10. Subfraction A4.2 consists of pinostrobin (PN). Further purification of subfraction A4.2 using CHCl₃: EtOAc in the ratio 8:2 to 0:1 gave subfractions A4.2.4 and A4.2.5 as NR and alpinone (AL), respectively (Fig. 1). The subfraction A5–A11 was not chosen to be purified because their intense red color indicated a high amount of brazilin or brazilin, which was reported as a major compound in *C. sappan* (Ngamwonglumlert *et al.*, 2020).

In vitro antioxidant activity using DPPH

The antioxidant activity test method followed the standard protocol with some modifications (Udenigwe *et al.*, 2009). All fractions and partitions were dissolved in methanol as a stock of 200 ppm. About 100 μl of each fraction/partition was added to the upper row of the 96-well costar microplate well, diluted stepwise until row 10, and followed by the addition of 100

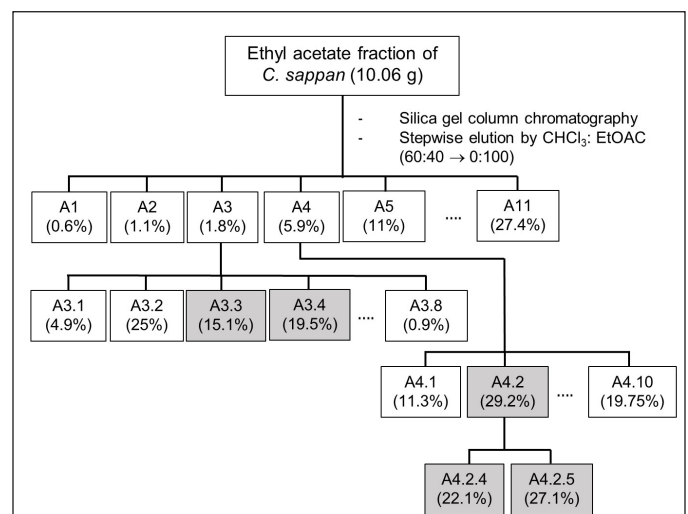


Figure 1. Purification of ethyl acetate fraction of *C. sappan*.

μl DPPH (0.1 mM) in each well. DPPH solution and methanol were added in rows 11 and 12, respectively. The mixture was incubated for 30 minutes at room temperature. The absorbance of each fraction was analyzed using a microplate reader at 517 nm without shaking. Ascorbic acid (AA) was used as a positive control. DPPH radical scavenging ability was measured using the following equation:

$$\% \text{Inhibitor} = \left(\frac{A_c - A_s}{A_c} \right) \times 100 \%$$

where A_c is the absorbance of the control containing DPPH solution and A_s is the absorbance of the sample. The IC_{50} value was calculated from $y = ax \pm b$ obtained from plotting a graph between %inhibitors (y -axis) and concentrations (x -axis).

Chemical constituent analysis using LC-QToF-MS/MS

The identification methods of the molecules were performed by LC-QToF-MS/MS, which was conducted in the Forensic Laboratory of Indonesia National Police. The analysis used a C_{18} column (1.8 μm, 2.1 × 100 mm) with an injection volume of 5 μl. The combination of water + 5 mM ammonium formic and acetonitrile + 0.05% formic acid was used. The conditions of the column were as follows: column temperature = 50°C, flow rate = 0.2 ml/minute, and 23 minutes of running. Electrospray ionization was used to elucidate the compounds, with a positive mode of detection, mass analysis range = 50–1,200 m/z , source temperature = 100°C, desolvation temperature = 350°C, collision energy = 4 volts, and ramp collision energy = 25–60 volts. The mzCloud Library was used to analyze the proposed compounds from *C. sappan* extract. From this analysis, subfraction A3.3 was recorded as 2',5,6-TM and subfraction A3.4 as CR; subfraction A4.2 consisted of PN; subfraction A4.2.4 was identified as NR and subfraction A4.2.5 as AL (Fig. 1).

Molecular docking and molecular dynamics (MDs) studies

All ligands were collected from PubChem in 3D .sdf format and converted to .pdb using Discovery Studio 2019. CP450 (PDB id: 1OG5), LO (1N8Q), NO (2CDU), and XO (3NRZ) macromolecules were retrieved from www.rcsb.org and optimized using Schrodinger Maestro 11.8. Autodocktools 1.5.6 was used for docking all ligands with their receptors. Water residue in the receptors was removed, and Kollman charge was added to the macromolecules. Docking was repeated several times to get root mean square deviation (RMSD) <2 Å (Rizvi *et al.*, 2013). Discovery Studio was used to visualize 2D and 3D interactions

between ligands and receptors. The same procedure was also applied for native ligands/controls.

The ligand topology for MDs was prepared using PRODRG and MD and conducted on <https://simlab.uams.edu/> with adjusted parameters such as a temperature of 300 K, 20 ns simulation time, 0.15 M NaCl, GROMOS96 43a1 for forcefield, and pressure at 1 atm (Bekker *et al.*, 1993; Schüttelkopf and van Aalten, 2004).

The bond dissociation energy (BDE) and bond dissociation free energy (BDFE) of each –OH from flavone and flavanone derivatives were calculated using density functional theory (DFT) on www.bde.ml.nrel.gov (St. John *et al.*, 2020).

Statistical analysis

The data presented in the figures are representative of three independent analyses that gave similar results. The values are presented as the means ± SD. The differences between data were analyzed using Student's *t*-test. The statistical significance was set at $p < 0.05$ and $p < 0.01$.

RESULT AND DISCUSSION

Extraction and fractionation of *C. sappan*

Dried simplisia of *C. sappan* extracted using MeOH gave 10.2% of crude extract. Fractionation of the crude extract using ethyl acetate (hydrophobic solvent) afforded 74.0% of fraction A. Based on the radical scavenging activity test using the DPPH method, the constituents in fraction A supposed to have potency as antioxidants, shown by the $IC_{50} = 0.36 \pm 0.03$ μg/ml (very strong category) (Riza Marjoni and Zulfisa, 2017). Purification of fraction A carried out by SiO₂ open column chromatography gave subfractions A1–A11. Among them, subfractions A3 and A4 are our subjects of interest based on their antioxidant activities. Subfractions A5–A11 collected as a powder with an intense red color suggested the major constituents should be brazilin or brazilin (Ngamwonglumlert *et al.*, 2020).

The purification of subfractions A3 and A4 is depicted in Figure 1. Five compounds consisting of subfractions A3.3, A3.4, A4.2, A4.2.4, and A4.2.5 are determined as classes of flavone and flavanone, that is, 2',5,6-TM, CR, PN, NR-5-methyl ether, and AL determined by LC-MS/QToF (Table 1). The structures are depicted in Figure 2. All the detected compounds have similar parent fragments to those in previous studies. The 2',5,6-TM has a molecular formula $C_{18}H_{16}O_5$ with m/z 312.1074 (M+H)⁺ as reported by Wollenweber *et al.* (1990). CR ($C_{17}H_{14}O_6$) was found with m/z 314.0880 (M+H)⁺, as published by Suleimenov *et al.* (2008). PN

Table 1. LC-MS/QToF analysis of flavone and flavanone class compounds.

Compound	Experimental (m/z)	Calculated (m/z)	Relative peak area (%)				
			A3.3	A3.4	A4.2	A4.2.4	A4.2.5
2',5,6-TM	312.1074	312.1076	6.67	-	-	-	-
CR	314.0880	314.0869	-	5.01	-	-	-
PN	270.0970	270.0970	-	-	28.30	-	-
NR-5-methyl ether	286.0913	286.0919	-	-	-	11.71	-
AL	286.0930	286.0919	-	-	-	-	38.03

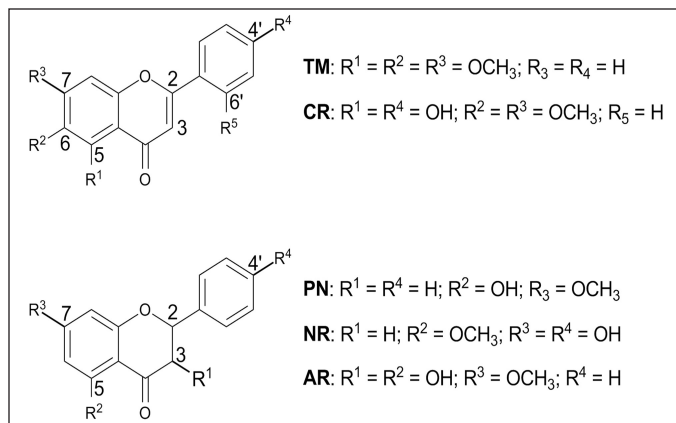


Figure 2. Structure of the identified compounds.

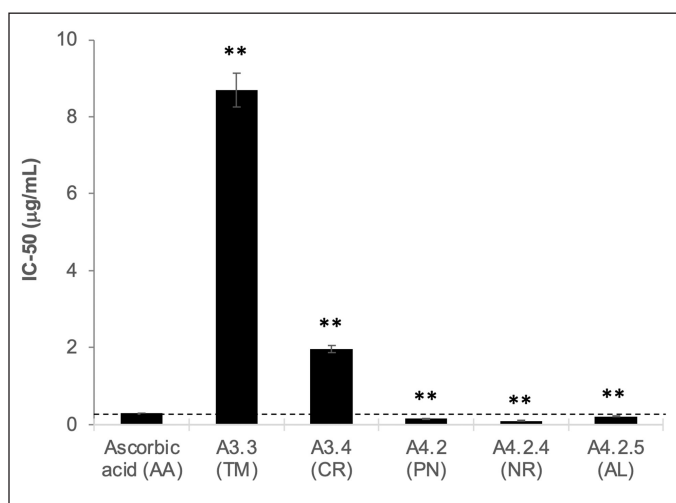


Figure 3. Antioxidant activity of subfraction based on the IC₅₀ analysis using the DPPH method. The data represent the mean ± SD (*n* = 3). ***p* < 0.01 and **p* < 0.05.

(C₁₆H₁₄O₄) was found with *m/z* 270.0972 (M+H)⁺, similar to the results in the report by Hua *et al.* (2011). NR-5-methyl ether with the molecular formula (C₁₆H₁₄O₅) with *m/z* 287.0913 (M+H)⁺ has the same fragment as that published in Hammami *et al.* (2004). AL (C₁₆H₁₄O₅) was established to have *m/z* 287.0930 (M+H)⁺ in agreement with Singh *et al.* (2019).

In vitro antioxidant activity of the isolated compounds

The antioxidant activity of subfractions A3.3, A3.4, A4.2, A4.2.4, and A4.2.5 was performed using the DPPH method and compared with AA as a positive control (Fig. 3). Subfractions A4.2 (IC₅₀ = 0.15 ± 0.02 µg/ml), A4.2.4 (IC₅₀ = 0.10 ± 0.03 µg/ml), and A4.2.5 (IC₅₀ = 0.21 ± 0.01 µg/ml) have comparable IC₅₀ values to that of AA (IC₅₀ = 0.29 ± 0.02 µg/ml). Thus, it is suggested that the major constituent in these subfractions should be responsible for stabilizing free radicals. Subfractions A3.3 and A3.4 showed a higher IC₅₀ than that of AA, but in general, they possess a very strong antioxidant property (Riza Marjoni and Zulfisa, 2017). From the LC-MS analysis, PN (28.30%) is the major compound from A4.2, contributing to its antioxidant activity because it has a hydroxyl group. PN was analyzed for its antioxidant activity, with

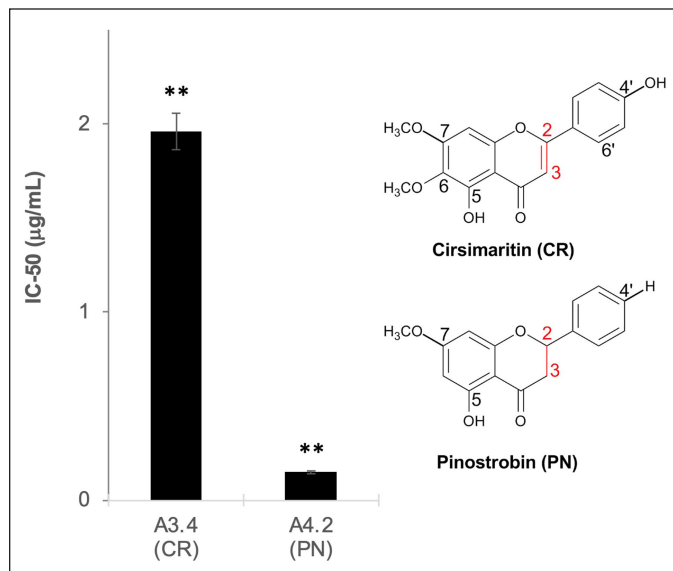


Figure 4. Effect of the presence of π-bond at C₂=C₃ on flavone and flavanone. The data represent the mean ± SD (*n* = 3). ***p* < 0.01 and **p* < 0.05.

IC₅₀ > 500 µg/ml against DPPH (Christov *et al.*, 2005). NR is a potent antioxidant agent due to its ability to scavenge hydroxyl, hydrogen peroxide, superoxide, and nitric oxide radicals (Rashmi *et al.*, 2018). The NR 5-methyl is suspected of having similar antioxidant activities to the reported data.

The variation of the substituent in the core structure of flavone (A3) and flavanone (A4) gives different activities for radical trapping. Comparing the kind and the position of substituent give useful insight for SAR analysis. Three cases were evaluated based on structural differences, as follows: (1) the presence of π-bond at C₂=C₃ in flavone and flavanone; (2) the presence of OH in flavone; and (3) the presence of OH in aromatic ring (A and B) in flavanone.

From Figure 4, PN in A4.2 exerts better scavenging ability than A3.4 with this only one hydroxyl at rge C5 position attached to PN. In this case, it seems that there is no contribution to antioxidant activity from the extended conjugation system in the ring B and C by the presence of a double bond at the C₂=C₃ position on the CR (Wang *et al.*, 2018). Even though the IC₅₀ value of PN is lower than that of CR, CR still has a low IC₅₀ value, which might be caused by the methoxyl substituent at C₇ and C₆ (Sarian *et al.*, 2017).

Comparing the structures of TM and CR in the subfractions A3.3 and A3.4 showed that TM did not have any hydroxyl in the ring (Fig. 5). In contrast, CR has two hydroxyls attached in C₅ (ring A) and C₄' (ring B), which are supposed to contribute to their antioxidant activities by the HAT mechanism (Liang and Kitts, 2014). Two hydroxyl groups at ring A and ring B of flavonoids have been reported to exert higher antioxidant activity when compared to one hydroxyl group in either ring (Wang *et al.*, 2018). On the other hand, the *O*-methylation at the C₅ position in TM weakens its scavenging ability (Sarian *et al.*, 2017). For this reason, TM has a lower IC₅₀ than that of CR.

The PN, NR, and AL structures are the major flavonoid compounds in A4 and their subfractions. Among those compounds, NR ranks one as an antioxidant because two hydroxyl groups

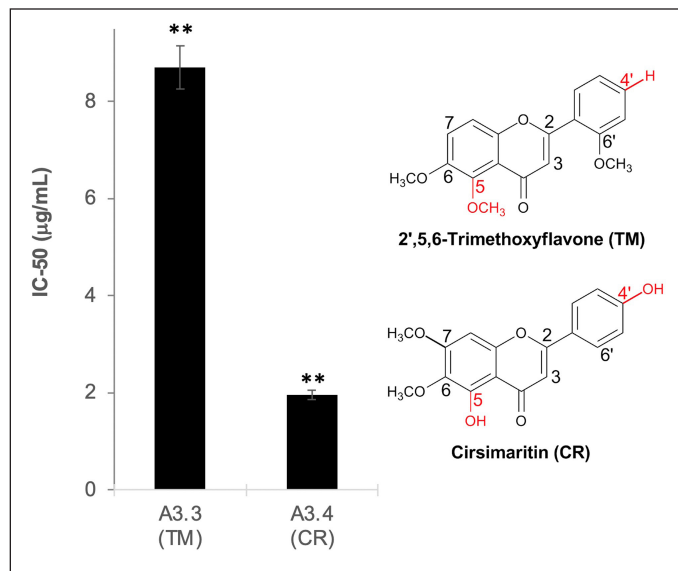


Figure 5. The effect of the presence of OH in flavone. The data represent the mean ± SD (*n* = 3). ***p* < 0.01 and **p* < 0.05.

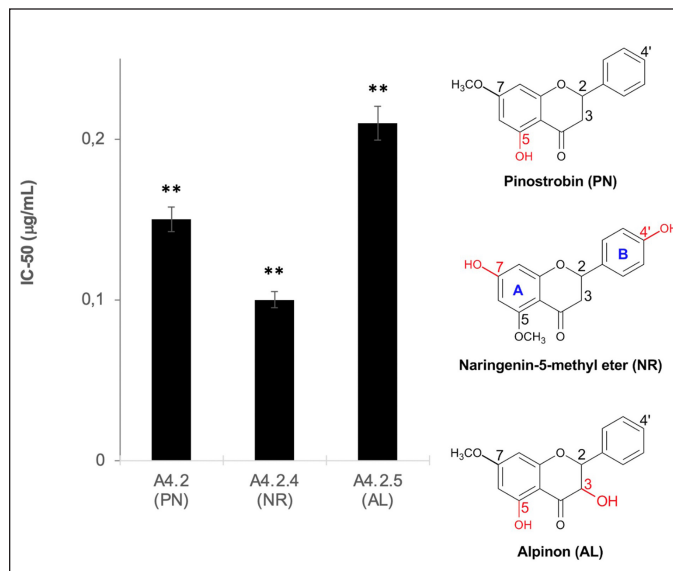


Figure 6. The effect of the presence of OH in aromatic ring (A and B) in flavanone. The data represent the mean ± SD (*n* = 3). ***p* < 0.01 and **p* < 0.05.

Table 2. BDE and BDFE of flavone and flavanone from *C. sappan*.

Structure	Compounds	OH group position	BDE (kcal/mol)	BDFE (kcal/mol)
 Flavone	TM	-	-	-
	CR	<i>R</i> ¹ <i>R</i> ⁴	94.8 87.5	85.9 79.2
 Flavanone	PN	<i>R</i> ²	93.1	84.5
	NR	<i>R</i> ³ <i>R</i> ⁴	89.4 87.5	81.1 79.2
	AL	<i>R</i> ¹ <i>R</i> ²	108.8 93.2	100.3 84.5

at ring A (C-7) and B (C-4') contribute the most to its activity (Fig. 6). However, AL also has two hydroxyls at C-3 and C-5 and supposedly has comparable antioxidant activity with NR. In fact, the BDE calculation of the hydroxyl in AL is 93.2–108.8 kcal/mol higher than that in NR, suggesting that the hydrogen transfer from AL to the DPPH radical is more difficult (Vo *et al.*, 2019). The order of easiness of hydrogen transfer is NR>PN>AL, and this result is supported by *in vitro* (Fig. 6) and DFT calculation (Table 2). Further detailed investigation of *in vitro* analysis and apoptosis using cell lines is in progress.

In silico study of the isolated compounds

The known enzyme that generates ROS is CP450, 5-LO, NO, and XO (Dharmaraja, 2017). Prior to molecular docking, a validation method is needed to see whether the applied method reproduces valid data compared with the published one. The RMSD values between the calculated and experimental X-ray crystallographic data must be less than 2.0 Å to be considered a

success (Hevener *et al.*, 2009). The similarity of conformation between the calculated (blue) and from this experiment (yellow) was tested using molecular docking protocol (Fig. 7). Co-crystal ligands were chosen in this validation due to their inhibition of the macromolecules' active sites. If the result shows that the RMSD of all receptors is less than 2.0 Å, then the method is validated.

The SARs of TM, CR, PN, NR, and AL are analyzed using those enzymes. First, the analysis suggested that all the identified compounds were able to inhibit the active site of the receptors and have similar or better binding free energy compared to the cocrystal ligands, except for LO (Fig. 8).

The study about the S-warfarin complex with CYP450 reveals a new active site, including the interaction with Arg97, Gly98, Ile99, Phe100, Leu102, Ala103, Val113, Phe114, Asn217, Thr364, Ser365, Leu366, Pro367, and Phe476 residues (Williams *et al.*, 2003). Figure 9 shows that all flavonoid compounds have better binding free energy than 5-fluorouracil (FLU). CR has the best binding energy because it interacts with

CP450 residues via a hydrogen bond, but most interactions are not similar to those of S-warfarin. The hydroxyl group in the C7

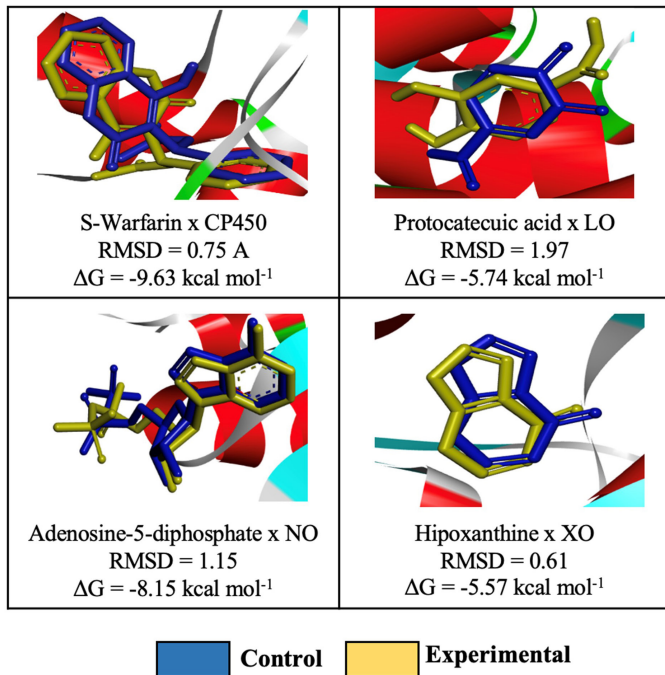


Figure 7. Molecular docking protocol validation for the receptors: CP450, LO, NO, and XO.

and C4' of NR helps to inhibit the active site by interacting with key residues, such as Val113 and ASN217. For the flavone ring, –OCH₃ in the R² position enables it to interact with Phe476, while –OH from CR at R⁴ interacts with Gly98. The hydroxyl group from PN (R¹) interacts with Ala103. From the MD simulation, the most stable ligand is AL with RMSD around 2 Å (Fig. 10).

Quercetin is a known potent inhibitor of the LO enzyme because of its competitive inhibition. The crucial residues that quercetin interacts with are His523 and Gln514 via a hydrogen bond (Borbulevych *et al.*, 2004). The only drug commercially available that can inhibit LO is zileuton (ZIL) (Rossi *et al.*, 2010). In this study, ZIL can interact with His523 and Gln514 by pi-pi T-shaped and hydrogen bonds, respectively. The identified flavonoids from *C. sappan* only inhibit either one of them, so they are not a good candidate as a LO inhibitor. CR and AL are excluded from Figures 10 and 11 because of their low binding energy. But the interesting part is the hydroxyl group at the C3 position of AL ($\Delta G = -1.7$ kcal/mol) is negligible in the active site of LO because, without the hydroxyl group at the C3 position, the binding free energy of PN ($\Delta G = -4.05$ kcal/mol) is better. Both –OCH₃ from TM (R¹) and NR (R²) interact with His523 via pi-sigma and are stable at 2.4 Å from the MD result (Fig. 10).

Adenosine 5-diphosphate (ADP) is a ligand that occupies the binding site of NO. The residues that interact with the ADP molecule are Ile160, Tyr159, Tyr188, Asp179, and His181. ADP acts as an H₂O₂ blocker, so the hydrogen peroxide will stay inside the complex NO and not dissociate from it (Lountos *et al.*, 2006). All the compounds inhibit the same active

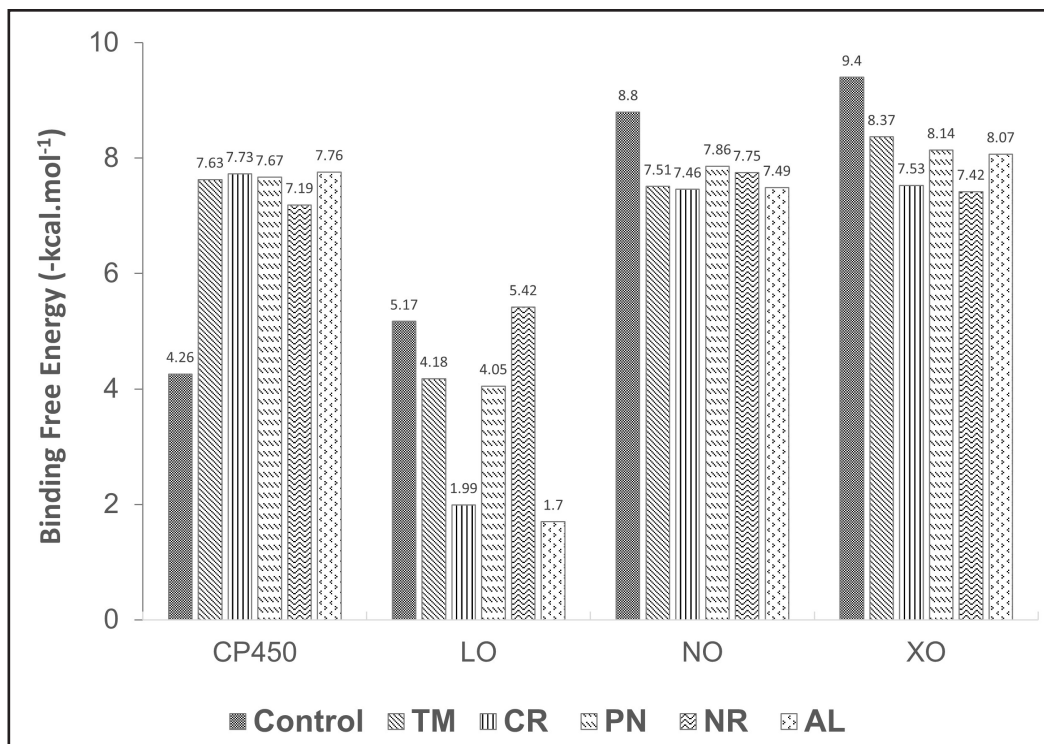


Figure 8. Binding energy values generated by molecular docking between ligands and receptors. Control molecules for C450, LO, NO, and XO were 5-FLU, ZIL, DEX, and FEB, respectively.

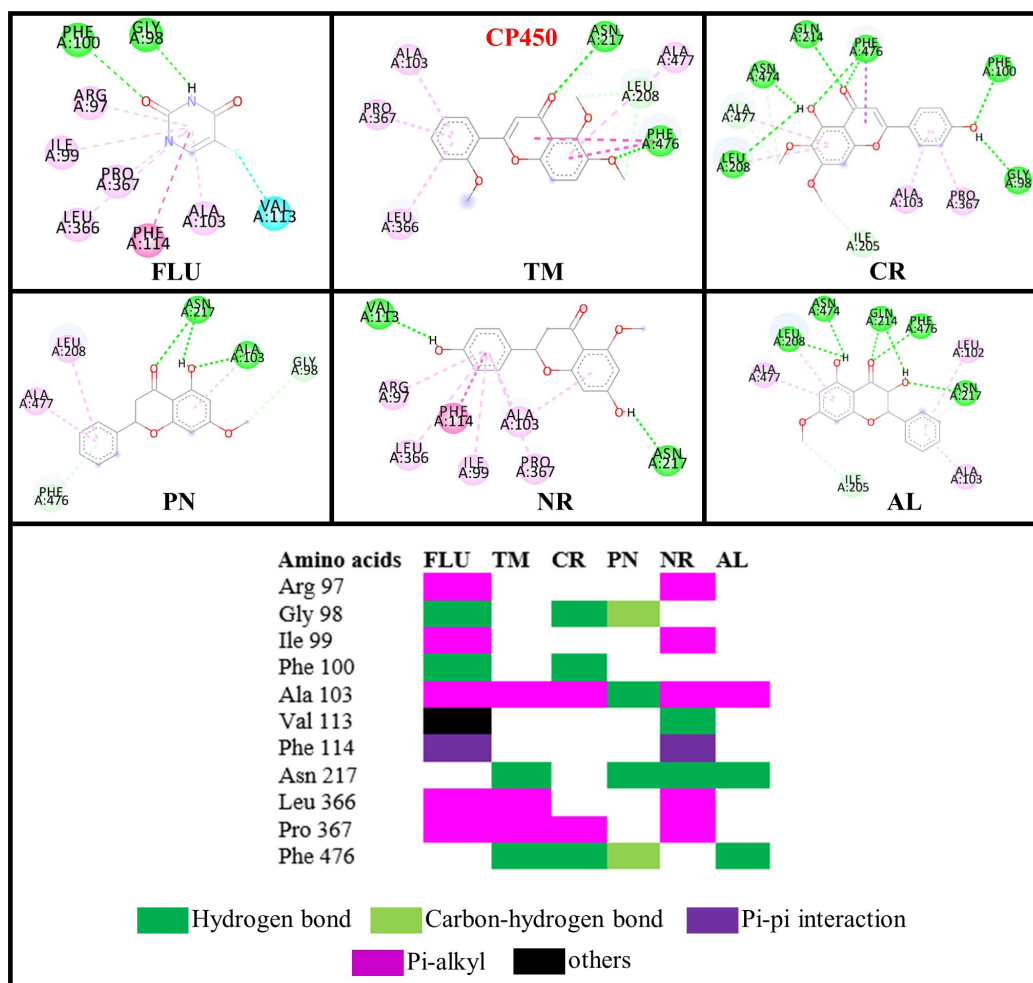


Figure 9. Interactions of the flavonoid and control (FLU) compounds against the CP450 receptor.

site and interact similarly with amino acid residues as ADP (Fig. 12). Dextromethorphan (DEX) is a known NO inhibitor with $\Delta G = -8.88 \text{ kcal/mol}^{-1}$, but it only interacts with Ile160 and Tyr188 (Chen *et al.*, 2018). The similarity of TM and CR to ADP is better than DEX because the methoxy group interacts with the residues in the active site. The double bond C2=C3 in flavone supports the interaction with Asp179. AL has the most hydrogen bond interaction due to hydroxyl groups, which increases the stability of the complex, but it does not help interact with the important residues (Majewski *et al.*, 2019). However, the $-\text{OCH}_3$ from TM interacts with Tyr188, which might contribute to the stability of TM inside the active site of NO with RMSD around 2 Å (Fig. 10).

XO generates ROS in our body while converting hypoxanthine to xanthine by the hydroxylation reaction (Kalra *et al.*, 2007). Glu 802, Glu1261, and Arg880 are critical residues for substrate hydroxylation. A known XO inhibitor like febuxostat (FEB) has been proven to interact with Glu802, Arg880, Thr1010, and Asn768 (Šmelcerović *et al.*, 2017). In this experiment, FEB only interacts with Arg880, Thr1010, and Asn768 because of the different molecular docking programs used in the literature (Liu *et al.*, 2022). All the flavonoid compounds do not interact

with Glu802, but most interact with Glu1261, except folerogenin (Fig. 13). TM shows the best binding free energy ($\Delta G = -8.37 \text{ kcal/mol}^{-1}$) because it interacts with two essential residues. The methoxy group of TM at the C-6 position is an important functional group because it interacts with Arg880. To interact with Arg880, the flavonoid compounds must have two methoxy groups at the C-6 and C-5 positions, like TM. From the MD result, TM is relatively stable below 2 Å until 5 ns, but it changes its position after that (Fig. 10).

From Table 3, the antioxidant activities of flavonoids can be enhanced by altering the position of $-\text{OH}$ and $-\text{OCH}_3$ groups. In the flavanone structure, the hydroxyl group is crucial for contacting key residues in CP and XO. In this experiment, two $-\text{OH}$ groups of NR interact with important residues in those macromolecules, unlike AL. This result correlates with the data obtained from the DPPH method. When comparing *in vitro* and *in silico* data, two hydroxyl groups of NR outweigh the ability to scavenge DPPH radicals in the O-methylation groups in TM (Moalin *et al.*, 2011). However, according to MD and molecular docking results, the methoxy groups of TM have better interactions by inhibiting crucial residues than the $-\text{OH}$ from NR.

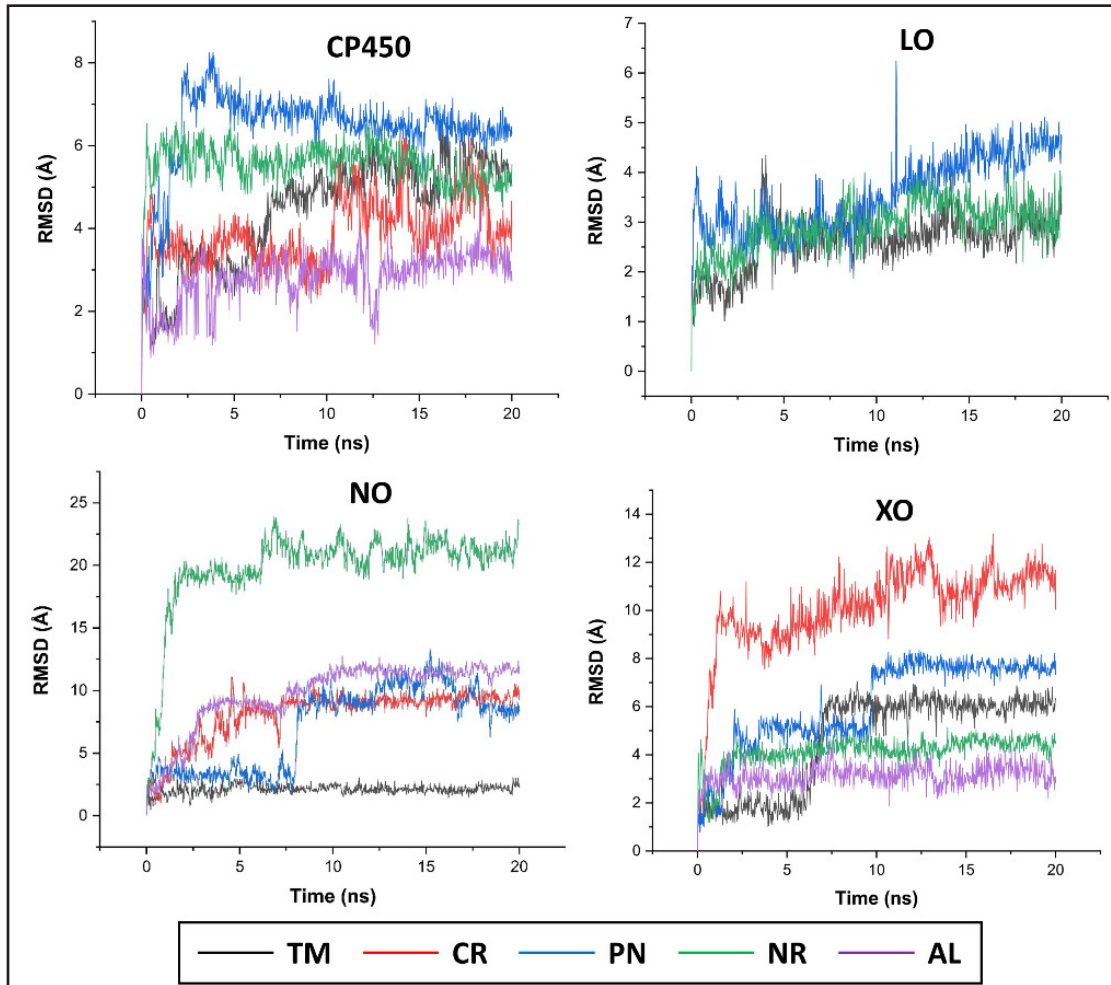


Figure 10. MDs simulation of RMSD ligand movement.

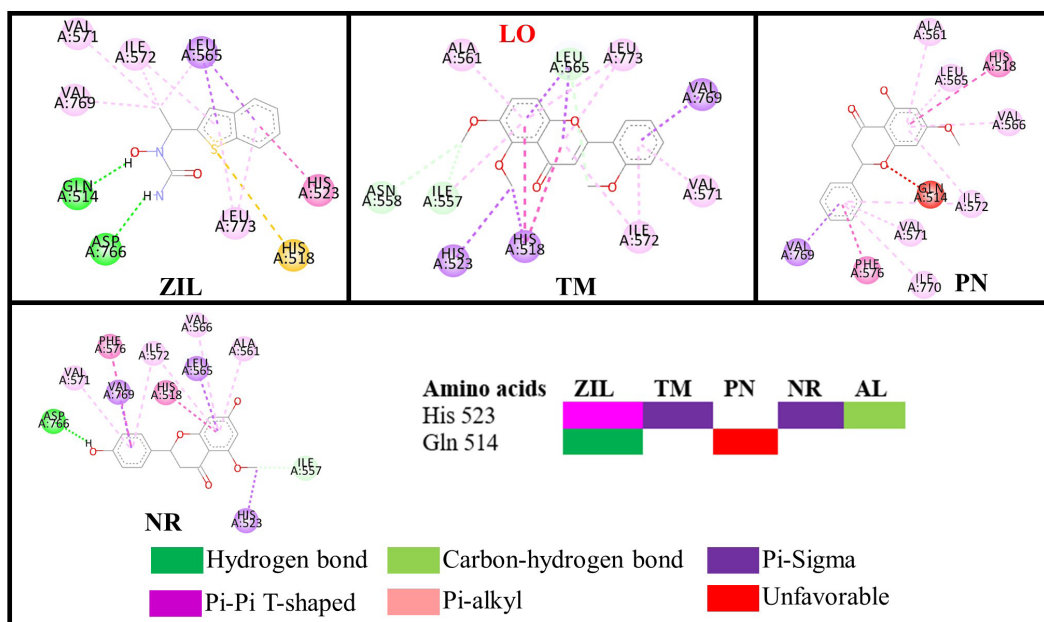


Figure 11. Interactions of the flavonoid and control (ZIL) compounds against the LO receptor.

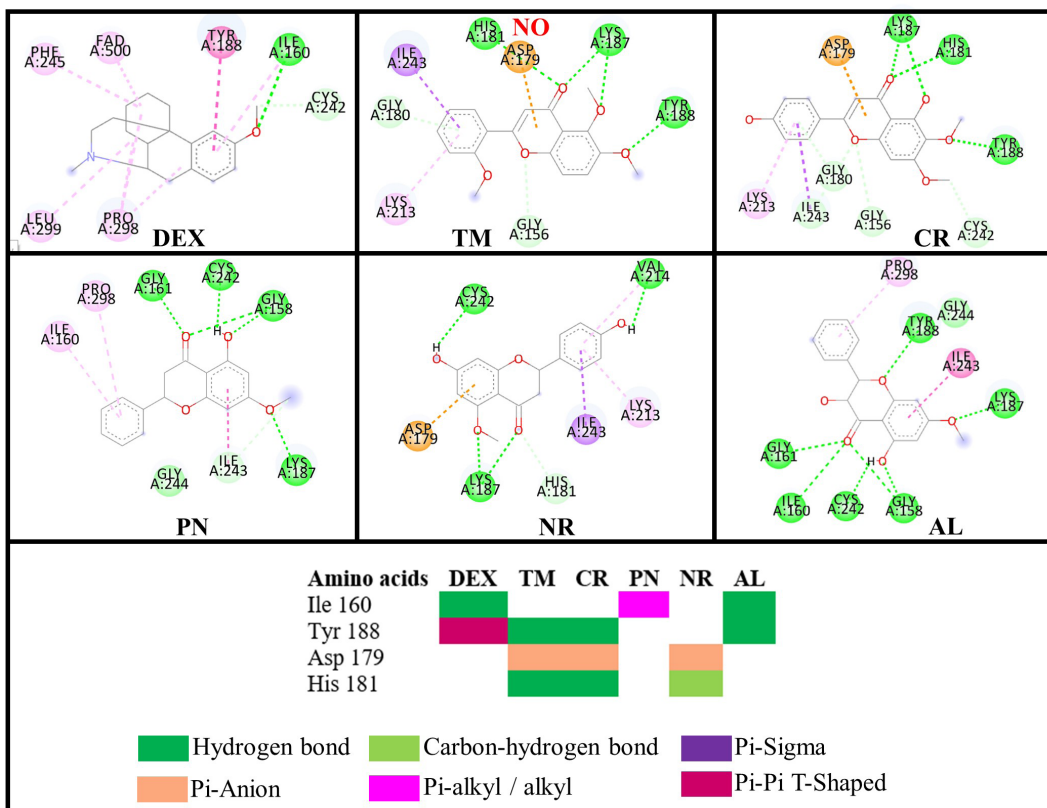


Figure 12. Interactions of the flavonoid and control (DEX) compounds against the NO receptor.

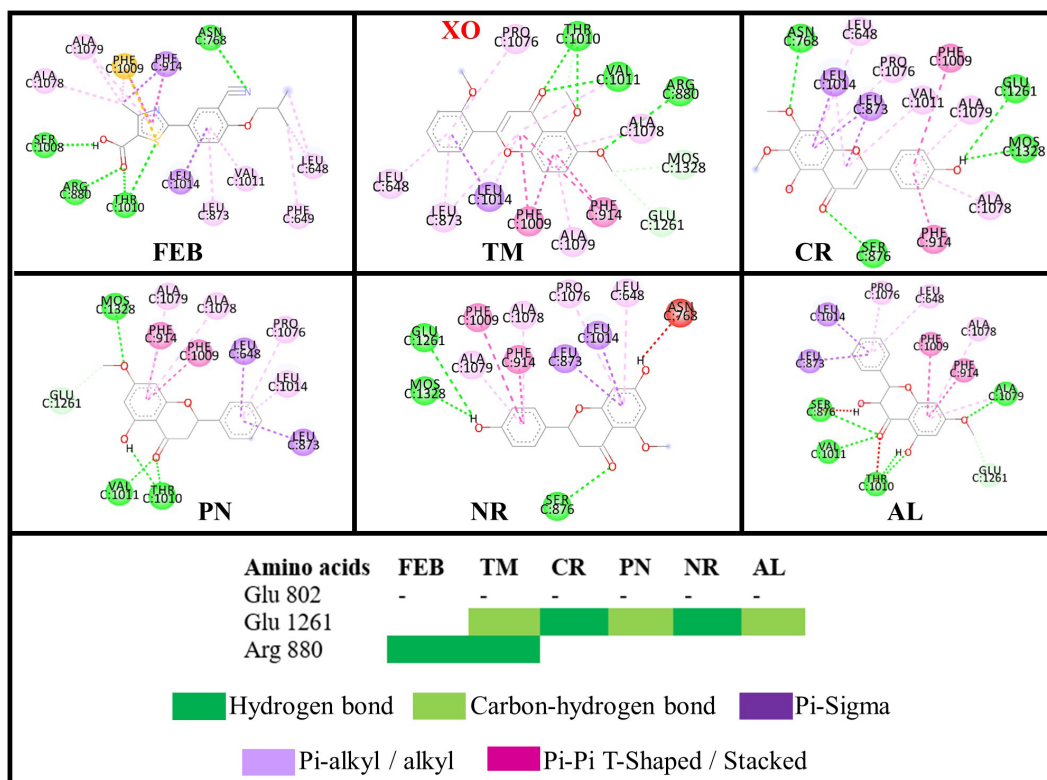
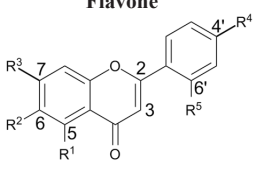
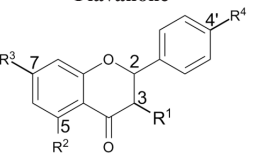


Figure 13. Interactions of the flavonoid and control (FEB) compounds against the XO receptor.

Table 3. Interactions between functional groups in flavon and flavanone against prooxidant enzymes.

Structure	R-	Interaction with key residues in			
		CP	LO	NO	XO
 <p>Flavone</p>	R1	-	-OCH ₃ (His523)	-	-
	R2	-OCH ₃ (Phe476)	-	-OCH ₃ (Tyr188)	-OCH ₃ (Arg880)
	R3	-	-	-OCH ₃ (Cys242)	-
	R4	-OH (Gly98)	-	-	-OH (Glu1261)
	R5	-	-	-	-
	C2=C3	-	-	Asp179	-
 <p>Flavanone</p>	R1	-OH (Ala103)	-	-	-
	R2	-OCH ₃ (Phe476)	-OCH ₃ (His523)	-	-
	R3	-OH (Asn217)	-	-	-OCH ₃ (Glu1261)
	R4	-OH (Val113)	-	-	-OH or -OCH ₃ (Glu1261)

CONCLUSION

This study revealed that the ethyl acetate fraction of *C. sappan* heartwood extract has high antioxidant activity because it contains a class of flavonoids. Among the flavones and flavanones isolated are 2',5,6-TM, CR, PN, NR-5-methyl ether, and AL determined by LC- QToF-MS/MS. The SAR analysis using molecular docking study tentatively suggested that the position of hydroxyl groups, pi-bonding at C2=C3, and methoxy groups in flavone or flavanone affect their inhibition and stabilities against the prooxidant enzymes by interacting with key residues. Further research will be conducted, including the purification of flavone and flavanone from *C. sappan* and testing those compounds to the related enzymes to fully understand the SAR of flavonoids isolated from *C. sappan* as antioxidant agents.

ACKNOWLEDGMENT

This research is financially supported by HPU research funding No. 975.32/UN10.C10/PN/2022 from Brawijaya University.

AUTHOR CONTRIBUTIONS

All authors made substantial contributions to conception and design, acquisition of data, or analysis and interpretation of data; took part in drafting the article or revising it critically for important intellectual content; agreed to submit to the current journal; gave final approval of the version to be published; and agree to be accountable for all aspects of the work. All the authors are eligible to be an author as per the international committee of medical journal editors (ICMJE) requirements/guidelines.

CONFLICTS OF INTEREST

The authors report no financial or any other conflicts of interest in this work.

ETHICAL APPROVALS

This study does not involve experiments on animals or human subjects.

DATA AVAILABILITY

All data generated and analyzed are included in this research article.

PUBLISHER'S NOTE

This journal remains neutral with regard to jurisdictional claims in published institutional affiliation.

REFERENCES

- Amić D, Davidović-Amić D, Beslo D, Rastija V, Lucić B, Trinajstić N. SAR and QSAR of the antioxidant activity of flavonoids. *Curr Med Chem*, 2007; 14:827–45.
- Annamalai S, Arumugam S, Venugopal A, Kumar S, Jkkmmrf's-Annai N, Sampoorani J. Evaluation of anti-diabetic activity of *Caesalpinia sappan* wood against alloxan induced diabetic rats. *Int J Pharm Health Care Res*, 2019; 2:184–91.
- Arjin C, Hongsibsong S, Pringproa K, Seel-Audom M, Ruksiriwanich W, Sutan K, Sommano SR, Sringarm K. Effect of ethanolic *Caesalpinia sappan* fraction on *in vitro* antiviral activity against porcine reproductive and respiratory syndrome virus. *Vet Sci*, 2021; 8:106.
- Badami S, Moorkoth S, Rai SR, Kannan E, Bhojraj S. Antioxidant activity of *Caesalpinia sappan* heartwood. *Biol Pharm Bull*, 2003; 26:1534–7.
- Bekker H, Berendsen H, Dijkstra EJ, Achterop S, Drunen R, van der Spoel D, Sijbers A, Keegstra H, Renardus MKR. Gromacs: a parallel computer for molecular dynamics simulations. *Phys Comput*, 1993; 92:252–6.
- Bhattacharyya A, Chattopadhyay R, Mitra S, Crowe SE. Oxidative stress: an essential factor in the pathogenesis of gastrointestinal mucosal diseases. *Physiol Rev*, 2014; 94:329–54.
- Borbulevych OY, Jankun J, Selman SH, Skrzypczak-Jankun E. Lipoygenase interactions with natural flavonoid, quercetin, reveal a complex with protocatechuic acid in its X-ray structure at 2.1 Å resolution. *Proteins*, 2004; 54:13–9.
- Chen CL, Cheng MH, Kuo CF, Cheng YL, Li MH, Chang CP, Wu JJ, Anderson R, Wang S, Tsai PJ, Liu CC, Lin YS. Dextromethorphan attenuates NADPH oxidase-regulated glycogen synthase kinase 3β and NF-κB activation and reduces nitric oxide production in group A streptococcal infection. *Antimicrob Agents Chemother*, 2018; 62:e02045–17.
- Christov R, Trusheva B, Popova M, Bankova V, Bertrand M. Chemical composition of propolis from Canada, its antiradical activity and plant origin. *Nat Prod Res*, 2005; 19:673–8.
- Cuong TD, Hung TM, Kim JC, Kim EH, Woo MH, Choi JS, Lee JH, Min BS. Phenolic compounds from *Caesalpinia sappan* heartwood and their anti-inflammatory activity. *J Nat Prod*, 2012; 75:2069–75.
- Dahri M, Alghrably M, Mohammed HA, Badshah SL, Noreen N, Mouffouk F, Rayyan S, Qureshi KA, Mahmood D, Lachowicz JI, Jaremko M, Emwas AH. Natural polysaccharides as preventive and therapeutic horizon for neurodegenerative diseases. *Pharmaceutics*, 2022; 14:1.
- Dharmaraja AT. Role of reactive oxygen species (ROS) in therapeutics and drug resistance in cancer and bacteria. *J Med Chem*, 2017; 60:3221–40.

- Hammami S, Ben Jannet H, Bergaoui A, Ciavatta M, Cimino G, Gannoun S. Isolation and structure elucidation of a flavanone, a flavanone glycoside and vomifoliol from *Echiochilon fruticosum* growing in Tunisia. *Mol Basel Switz*, 2004; 9:602–8.
- He L, He T, Farrar S, Ji L, Liu T, Ma X. Antioxidants maintain cellular redox homeostasis by elimination of reactive oxygen species. *Cell Physiol Biochem*, 2017; 44:532–53.
- Hevener KE, Zhao W, Ball DM, Babaoglu K, Qi J, White SW, Lee RE. Validation of molecular docking programs for virtual screening against dihydropteroate synthase. *J Chem Inf Model*, 2009; 49:444–60.
- Hua X, Fu YJ, Zu YG, Zhang L, Wang W, Luo M. Determination of pinostrobin in rat plasma by LC-MS/MS: application to pharmacokinetics. *J Pharm Biomed Anal*, 2011; 56:841–5.
- Kalra S, Jena G, Tikoo K, Mukhopadhyay A. Preferential inhibition of xanthine oxidase by 2-amino-6-hydroxy-8-mercaptapurine and 2-amino-6-purine thiol. *BMC Biochem*, 2007; 8:8.
- Liang CH, Chan LP, Chou TH, Chiang FY, Yen CM, Chen PJ, Ding HY, Lin RJ. Brazilein from *Caesalpinia sappan* L. antioxidant inhibits adipocyte differentiation and induces apoptosis through caspase-3 activity and anthelmintic activities against *Hymenolepis nana* and *Anisakis simplex*. *Evid Based Complement Alternat Med*, 2013; 2013:e864892.
- Liang N, Kitts D. Antioxidant property of coffee components: assessment of methods that define mechanisms of action. *Mol Basel Switz*, 2014; 19:19180–208.
- Lim MY, Jeon JH, Jeong EY, Lee CH, Lee HS. Antimicrobial activity of 5-hydroxy-1,4-naphthoquinone isolated from *Caesalpinia sappan* toward intestinal bacteria. *Food Chem*, 2007; 100:1254–8.
- Liu Z, Ren Z, Zhang J, Chuang CC, Kandaswamy E, Zhou T, Zuo L. Role of ROS and nutritional antioxidants in human diseases. *Front Physiol*, 2018; 9:477.
- Liu X, Wu D, Liu J, Li G, Zhang Z, Chen C, Zhang L, Li J. Characterization of xanthine oxidase inhibitory activities of phenols from pickled radish with molecular simulation. *Food Chem X*, 2022; 14:100343.
- Lountos GT, Jiang R, Wellborn WB, Thaler TL, Bommaris AS, Orville AM. The crystal structure of NAD(P)H oxidase from *Lactobacillus sanfranciscensis*: insights into the conversion of O₂ into two water molecules by the flavoenzyme. *Biochemistry*, 2006; 45:9648–59.
- Majewski M, Ruiz-Carmona S, Barril X. An investigation of structural stability in protein-ligand complexes reveals the balance between order and disorder. *Commun Chem*, 2019; 2:1–8.
- Moalin M, van Strijdonck GPF, Beckers M, Hagemen GJ, Borm PJ, Bast A, Haenen GRMM. A planar conformation and the hydroxyl groups in the B and C rings play a pivotal role in the antioxidant capacity of quercetin and quercetin derivatives. *Molecules*, 2011; 16:9636–50.
- Mohammed HA. The valuable impacts of halophytic genus *Suaeda*; nutritional, chemical, and biological values. *Med Chem Shariqah United Arab Emir*, 2020; 16:1044–57.
- Mueller M, Weinmann D, Toegel S, Holzer W, Unger FM, Viernstein H. Compounds from *Caesalpinia sappan* with anti-inflammatory properties in macrophages and chondrocytes. *Food Funct*, 2016; 7:1671–9.
- Naik Bukke A, Nazneen Hadi F, Babu KS, Shankar PC. *In vitro* studies data on anticancer activity of *Caesalpinia sappan* L. heartwood and leaf extracts on MCF7 and A549 cell lines. *Data Brief*, 2018; 19:868–77.
- Ngamwonglumlert L, Devahastin S, Chiewchan N, Raghavan GSV. Color and molecular structure alterations of brazilein extracted from *Caesalpinia sappan* L. under different pH and heating conditions. *Sci Rep*, 2020; 10:12386.
- Ningsih FN, Okuyama T, To S, Nishidono Y, Okumura T, Tanaka K, Ikeya Y, Nishizawa M. Comparative analysis of anti-inflammatory activity of the constituents of the rhizome of *Cnidium officinale* using rat hepatocytes. *Biol Pharm Bull*, 2020; 43:1867–75.
- Nirmal NP, Panichayupakaranant P. Antioxidant, antibacterial, and anti-inflammatory activities of standardized brazilein-rich *Caesalpinia sappan* extract. *Pharm Biol*, 2015; 53:1339–43.
- Pham-Huy LA, He H, Pham-Huy C. Free radicals, antioxidants in disease and health. *Int J Biomed Sci IJBS*, 2008; 4:89–96.
- Putri BM, Sugiarto, Wasita B, Febrinasari RP. Antioxidant activity of ethanol extract of secang wood (*Caesalpinia sappan* L.), gotu kola (*Centella asiatica* L.), and their combinations with DPPH assay. *Int Conf Health Sci Technol ICOHETECH*, 2021; 2:45–9.
- Qureshi KA, Mohammed SAA, Khan O, Ali HM, El-Readi MZ, Mohammed HA. Cinnamaldehyde-based self-nanoemulsion (CA-SNEDDS) accelerates wound healing and exerts antimicrobial, antioxidant, and anti-inflammatory effects in rats' skin burn model. *Molecules*, 2022; 27:5225.
- Rashmi R, Bojan Magesh S, Mohanram Ramkumar K, Suryanarayananl S, Venkata SubbaRao M. Antioxidant potential of naringenin helps to protect liver tissue from streptozotocin-induced damage. *Rep Biochem Mol Biol*, 2018; 7:76–84.
- Riza Marjoni M, Zulfisa A. Antioxidant activity of methanol extract/fractions of senggani leaves (*Melastoma candidum* D. Don). *Pharm Anal Acta*, 2017; 08:8.
- Rizvi SMD, Shakil S, Haneef M. A simple click by click protocol to perform docking: autodock 4.2 made easy for non-bioinformaticians. *EXCLI J*, 2013; 12:831–57.
- Rossi A, Pergola C, Koeberle A, Hoffmann M, Dehm F, Bramanti P, Cuzzocrea S, Werz O, Sautebin L. The 5-lipoxygenase inhibitor, zileuton, suppresses prostaglandin biosynthesis by inhibition of arachidonic acid release in macrophages. *Br J Pharmacol*, 2010; 161:555–70.
- Sarian MN, Ahmed QU, Mat So'ad SZ, Alhassan AM, Murugesu S, Perumal V, Mohamad SNAS, Khatib A, Latip J. Antioxidant and antidiabetic effects of flavonoids: a structure-activity relationship based study. *BioMed Res Int*, 2017; 2017:8386065.
- Schüttelkopf AW, van Aalten DMF. PRODRG: a tool for high-throughput crystallography of protein-ligand complexes. *Acta Crystallogr D Biol Crystallogr*, 2004; 60:1355–63.
- Shu SH, Han JL, Du GH, Qin HL. A new flavonoid from heartwood of *Caesalpinia sappan*. *Zhongguo Zhong Yao Za Zhi*, 2008; 33:903–5.
- Singh P, Bajpai V, Sharma A, Singh B, Kumar B. Chemical profiling and discrimination of medicinal Himalayan *Iris* species using direct analysis in real time mass spectrometry combined with principal component analysis. *Br J Anal Chem*, 2019; 6:1–16.
- Šmelcerović A, Tomović K, Šmelcerović Ž, Petronijević Ž, Kocić G, Tomašić T, Jakopin Z, Anderluh M. Xanthine oxidase inhibitors beyond allopurinol and febuxostat; an overview and selection of potential leads based on *in silico* calculated physico-chemical properties, predicted pharmacokinetics and toxicity. *Eur J Med Chem*, 2017; 135:491–516.
- St. John PC, Guan Y, Kim Y, Kim S, Paton RS. Prediction of organic homolytic bond dissociation enthalpies at near chemical accuracy with sub-second computational cost. *Nat Commun*, 2020; 11:2328.
- Suleimenov E, Raldugin V, Adekenov S. Cirsimaritin from *Stizolophus balsamita*. *Chem Nat Compd*, 2008; 44:398.
- Tatipamula VB, Kukavica B. Phenolic compounds as antidiabetic, anti-inflammatory, and anticancer agents and improvement of their bioavailability by liposomes. *Cell Biochem Funct*, 2021; 39:926–44.
- Udenigwe CC, Lu YL, Han CH, Hou WC, Aluko RE. Flaxseed protein-derived peptide fractions: antioxidant properties and inhibition of lipopolysaccharide-induced nitric oxide production in murine macrophages. *Food Chem*, 2009; 116:277–84.
- Ulfa SM, Shirako S, Sato M, Dwijayanti DR, Okuyama T, Horie S, Watanabe J, Ikeya Y, Nishizawa M. Anti-inflammatory effects of anthraquinones of *Polygonum multiflorum* roots. *Bioact Compd Health Dis*, 2022; 5:136–48.
- Vo QV, Nam PC, Thong NM, Trung NT, Phan CTD, Mechler A. Antioxidant motifs in flavonoids: O–H versus C–H bond dissociation. *ACS Omega*, 2019; 4:8935–42.
- Wang T, Li Q, Bi K. Bioactive flavonoids in medicinal plants: structure, activity and biological fate. *Asian J Pharm Sci*, 2018; 13:12–23.

Williams PA, Cosme J, Ward A, Angove HC, Matak Vinković D, Jhoti H. Crystal structure of human cytochrome P450 2C9 with bound warfarin. *Nature*, 2003; 424:464–8.

Wollenweber E, Inuma M, Tanaka T, Mizuno M. 5-Hydroxy-6,2'-dimethoxyflavone from *Primula denticulata*. *Phytochemistry*, 1990; 29:633–7.

Yang S, Lian G. ROS and diseases: role in metabolism and energy supply. *Mol Cell Biochem*, 2020; 467:1–12.

How to cite this article:

Suchahyo A, Rahman MF, Khotimah H, Widodo W, Ulfa SM. Identification of flavone and flavanone from ethyl acetate fraction of *Caesalpinia sappan* heartwood and tentative structure - activity relationship: An *in vitro* and *in silico* approach. *J Appl Pharm Sci*, 2023; 13(11):089–100.